4

The QCD Pomeron

Following the success of the reggeization of various different elementary particles it was hoped that a particle could be identified with the quantum numbers of the Pomeron which would reggeize to give the Pomeron trajectory.

Unfortunately this turned out not to be possible. In particular, in QCD all the elementary particles carry colour so there is no basic QCD constituent with the quantum numbers of the Pomeron. In QCD the lowest order Feynman diagram that can simulate the exchange of a Pomeron is a two-gluon exchange diagram. This led Low (1975) to use two-gluon exchange as a model for the bare Pomeron. He made numerical estimates of the amplitude for the exchange of two gluons between two hadrons using the then fashionable bag model of hadrons. This was then developed by Nussinov (1975, 1976), who considered contributions from more than two exchanged gluons as well as uncrossed ladder corrections to the two-gluon exchange amplitude.

We have already implicitly used the Low–Nussinov model in Chapter 2 to construct the Pomeron in the scalar theory model considered in that chapter. Combining this with our experience in deriving the reggeized gluon we can see what the picture of the Pomeron is in leading logarithm perturbative QCD.

The imaginary part of the amplitude for Pomeron exchange is given in terms of the multi-Regge exchange amplitude for two incoming particles (quarks for simplicity) to scatter into two quarks plus n gluons. The difference between this imaginary part and the imaginary part of the reggeized gluon lies solely in the colour factor. In the Pomeron case a singlet of colour is exchanged in the t-channel.

At the tree level this amplitude is just the left hand side of a ladder graph with triple gluon vertices replaced by the effective

82

vertices, Γ, discussed in the preceding chapter. Loop effects are taken into account by replacing the vertical gluon lines of the ladder by reggeized gluons. In summary, the QCD Pomeron consists of a ladder whose vertical lines are reggeized gluons, with effective vertices, Γ, which couple the reggeized gluons and the rungs of the ladder, and with no colour carried up the ladder.

The Pomeron that is obtained has even charge conjugation, which means that it has the same coupling to quarks and to antiquarks. A trajectory with similar quantum numbers as the Pomeron but which has odd charge conjugation has been proposed by Bouquet *et al.* (1975) and Joynson *et al.* (1975) and is called the **odderon**. The lowest order diagram for odderon exchange is the exchange of three gluons in a colour singlet state. We shall not be considering the odderon in this book.

The famous Balitsky, Fadin, Kuraev, Lipatov (BFKL) equation is the integral equation which determines the behaviour of the Pomeron described above, in perturbative QCD. Several independent paths have led directly or indirectly to this integral equation. The method that we shall follow in this chapter is that of Fadin, Kuraev & Lipatov (1976) and Balitsky & Lipatov (1978).

4.1 First three orders of perturbation theory

Our task is to calculate, to leading $\ln s$, the amplitude for quark–quark elastic scattering, i.e. incoming quarks with momentum p_1, p_2 and helicity λ_1, λ_2 scatter into a final state of quarks with momentum $(p_1 - q), (p_2 + q)$ and helicity $\lambda_{1'}, \lambda_{2'}$, via the exchange of a colour singlet. Most of the work has already been done in the preceding chapter, when we considered the case of colour octet exchange in order to obtain the reggeized gluon. The difference arises in the colour factors. This chapter is therefore shorter and much less painful than the last!

Since we are interested in colour singlet exchange there is no contribution from the tree diagram Fig. 3.2. The lowest order which gives a non-trivial contribution is the one loop contribution shown in Fig. 3.4. In this case the colour factor is different from the case of the reggeized gluon. We project out the singlet

contribution so the colour factor of both graphs in Fig. 3.4 is

$$G_0^{(1)} = \frac{1}{N^2} \mathrm{Tr}(\tau_a \tau_b) \mathrm{Tr}(\tau_a \tau_b) = \frac{N^2 - 1}{4N^2}. \qquad (4.1)$$

Thus as can be seen from Eqs. (3.6) and (3.7) in the limit $|t| \ll s$ where $u \approx -s$, the real part of the amplitude cancels and we are left with a purely imaginary part which can be read off from Eq.(3.5):

$$\mathcal{A}_1^{(1)} = 4i\alpha_s^2 s \delta_{\lambda_1' \lambda_1} \delta_{\lambda_2' \lambda_2} G_0^{(1)} \int \frac{d^2\mathbf{k}}{\mathbf{k}^2(\mathbf{k} - \mathbf{q})^2}. \qquad (4.2)$$

Since the amplitude begins in order α_s^2 (with no $\ln s$ factor), i.e. order by order in perturbation theory the Pomeron exchange amplitude is suppressed by a power of $\ln s$ relative to the amplitude for the reggeized gluon exchange, it follows that the Pomeron has even signature. What we mean is that the amplitude for Pomeron exchange contains a signature factor:

$$\frac{1}{2}\left(1 + e^{i\pi\alpha_P(t)}\right),$$

where the Pomeron trajectory, $\alpha_P(t) = 1 + \mathcal{O}(\alpha_s)$. Expanding the above signature factor as a power series in α_s we see that the leading non-trivial order is imaginary and $\mathcal{O}(\alpha_s)$.

In the next order of perturbation theory the amplitude for colour singlet exchange has two components (as was the case for the reggeized gluon). The first component is given by (see Eq.(3.17))

$$\mathcal{A}_{2a}^{(1)} = i\frac{-g_{\sigma\tau}}{2} \int d(P.S.^3) \mathcal{A}_{2\to3}^{(8)\sigma}(k_1, k_2) \mathcal{A}_{2\to3}^{\dagger(8)\tau}(k_1 - q, k_2 - q), \quad (4.3)$$

but in this case the colour factor is given by

$$\frac{1}{N} \mathrm{Tr}(\tau_a \tau_b) \mathrm{Tr}(\tau_c \tau_d) f_{ace} f_{bde} = N G_0^{(1)}.$$

Thus from Eq.(3.22) we see that this gives us a contribution to the colour singlet amplitude:

$$\mathcal{A}_{2a}^{(1)} = -i\frac{2N\alpha_s^3}{\pi^2} \delta_{\lambda_1' \lambda_1} \delta_{\lambda_2' \lambda_2} G_0^{(1)} s \ln(s/\mathbf{k}^2) \int d^2\mathbf{k_1} d^2\mathbf{k_2}$$

$$\times \left[\frac{\mathbf{q}^2}{\mathbf{k_1}^2 \mathbf{k_2}^2 (\mathbf{k_1} - \mathbf{q})^2 (\mathbf{k_2} - \mathbf{q})^2} - \frac{1}{\mathbf{k_1}^2 (\mathbf{k_1} - \mathbf{k_2})^2 (\mathbf{k_2} - \mathbf{q})^2} \right.$$

$$\left. - \frac{1}{\mathbf{k_2}^2 (\mathbf{k_1} - \mathbf{q})^2 (\mathbf{k_1} - \mathbf{k_2})^2} \right]. \qquad (4.4)$$

The other component comes from the diagrams of Fig. 3.8. In the colour singlet case the colour factor is given by

$$\frac{1}{N^2}\mathrm{Tr}(\tau_a\tau_b\tau_c)\mathrm{Tr}(\tau_a\tau_b\tau_c) = \frac{N}{2}G_0^{(1)}.$$

So from Eq.(3.24) and this colour factor we see that the contribution from these graphs is

$$
\begin{aligned}
\mathcal{A}_{2b}^{(1)} &= -i\frac{N\alpha_s^3}{\pi^2}\delta_{\lambda_1'\lambda_1}\delta_{\lambda_2'\lambda_2}G_0^{(1)}s\,\ln\left(s/\mathbf{k}^2\right) \\
&\times \int d^2\mathbf{k_1}d^2\mathbf{k_2}\frac{1}{\mathbf{k_1^2}(\mathbf{k_1}-\mathbf{k_2})^2(\mathbf{k_2}-\mathbf{q})^2},
\end{aligned}\tag{4.5}
$$

with a similar contribution coming from the graphs with one gluon on the left of the cut.

We note that in this case we do *not* get a cancellation of the non-factorizing part and so we do *not* obtain an expression at the two-loop level which is proportional to the one loop amplitude. This is due to the different colour factors.

The total expression to order α_s^3 is therefore

$$
\begin{aligned}
\Im\mathrm{m}\mathcal{A}_2^{(1)} &= -\frac{2N\alpha_s^3}{\pi^2}s\,\delta_{\lambda_1'\lambda_1}\delta_{\lambda_2'\lambda_2}G_0^{(1)}\ln\left(s/\mathbf{k}^2\right)\int d^2\mathbf{k_1}d^2\mathbf{k_2} \\
&\times \left[\frac{\mathbf{q}^2}{\mathbf{k_1^2}\mathbf{k_2^2}(\mathbf{k_1}-\mathbf{q})^2(\mathbf{k_2}-\mathbf{q})^2}\right. \\
&\left. -\frac{1}{2}\frac{1}{\mathbf{k_1^2}(\mathbf{k_1}-\mathbf{k_2})^2(\mathbf{k_2}-\mathbf{q})^2} - \frac{1}{2}\frac{1}{\mathbf{k_2^2}(\mathbf{k_1}-\mathbf{k_2})^2(\mathbf{k_1}-\mathbf{q})^2}\right].
\end{aligned}\tag{4.6}
$$

It will once again prove to be convenient to work in terms of the Mellin transform of the amplitude and to this end we define a function $f(\omega, \mathbf{k_1}, \mathbf{k_2}, \mathbf{q})$ by

$$
\begin{aligned}
\int_1^\infty d\left(\frac{s}{\mathbf{k}^2}\right)\left(\frac{s}{\mathbf{k}^2}\right)^{-\omega-1}\frac{\mathcal{A}^{(1)}(s,t)}{s} &= 4i\alpha_s^2\delta_{\lambda_1'\lambda_1}\delta_{\lambda_2'\lambda_2}G_0^{(1)} \\
&\times \int\frac{d^2\mathbf{k_1}d^2\mathbf{k_2}}{\mathbf{k_2^2}(\mathbf{k_1}-\mathbf{q})^2}f(\omega,\mathbf{k_1},\mathbf{k_2},\mathbf{q})
\end{aligned}\tag{4.7}
$$

(note that the amplitude has been divided by s before the Mellin transform has been taken so that the leading order term has a Mellin transform proportional to $1/\omega$).
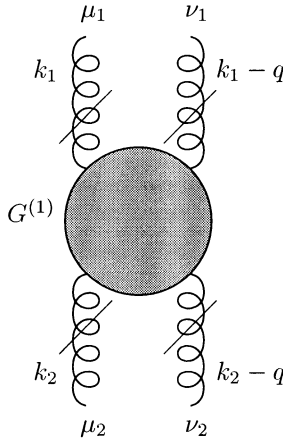
Fig. 4.1. Four-gluon Green function.

$f(\omega, \mathbf{k_1}, \mathbf{k_2}, \mathbf{q})$ is related to a Green function with four off-shell external gluons (see Fig. 4.1) by

$$\frac{f(\omega, \mathbf{k_1}, \mathbf{k_2}, \mathbf{q})}{\mathbf{k_2^2}(\mathbf{k_1} - \mathbf{q})^2} = \frac{s}{(2\pi)^4} \int d\rho_1 d\lambda_2 \frac{4p_1^{\mu_1} p_1^{\nu_1} p_2^{\mu_2} p_2^{\nu_2}}{s^2}$$

$$\times\ G_{\mu_1\mu_2\nu_1\nu_2}^{(1)}(\omega, k_1, k_2, q), \qquad (4.8)$$

where $G_{\mu_1\mu_2\nu_1\nu_2}^{(1)}(\omega, k_1, k_2, q)$ is the Mellin transform of the Green function for four external gluons with momenta $k_1, k_2, k_1 - q, k_2 - q$ with gluons 1 and 3 (2 and 4) being in a colour singlet state. These momenta can be expressed in terms of Sudakov variables ρ_1, λ_2 and their transverse components as

$$k_1^\mu = \rho_1 p_1^\mu - \frac{\mathbf{k_1^2}}{s} p_2^\mu + k_{1\perp}^\mu,$$

$$k_2^\mu = \frac{\mathbf{k_2^2}}{s} p_1^\mu + \lambda_2 p_2^\mu + k_{2\perp}^\mu,$$

$$q^\mu = \frac{\mathbf{q}^2}{s} p_1^\mu - \frac{\mathbf{q}^2}{s} p_2^\mu + q_\perp^\mu,$$

with $s\ (= 2p_1 \cdot p_2) \gg |\mathbf{q}^2|$. The integral over ρ_1, λ_2 is dominated by the region

$$\frac{\mathbf{k}^2}{s} \ll \rho_1, |\lambda_2| \ll 1.$$

The definition of $f(\omega, \mathbf{k_1}, \mathbf{k_2}, \mathbf{q})$ is somewhat different from the definition of $\mathcal{F}^{(8)}(\omega, \mathbf{k}, \mathbf{q})$ used in the case of the reggeized gluon, but has the advantage of being symmetric in $\mathbf{k_1}$ and $\mathbf{k_2}$ and can be viewed as a Green function.

Thus in leading (non-trivial) order of perturbation theory we have

$$f_1(\omega, \mathbf{k_1}, \mathbf{k_2}, \mathbf{q}) = \frac{1}{\omega}\delta^2(\mathbf{k_1} - \mathbf{k_2}) \tag{4.9}$$

and in the next order

$$f_2(\omega, \mathbf{k_1}, \mathbf{k_2}, \mathbf{q}) = -\frac{\bar{\alpha}_s}{2\pi}\frac{1}{\omega^2}$$
$$\times \left[\frac{\mathbf{q}^2}{\mathbf{k_1^2}(\mathbf{k_2} - \mathbf{q})^2} - \frac{1}{2}\frac{1}{(\mathbf{k_1} - \mathbf{k_2})^2}\left(1 + \frac{\mathbf{k_2^2}(\mathbf{k_1} - \mathbf{q})^2}{\mathbf{k_1^2}(\mathbf{k_2} - \mathbf{q})^2}\right)\right]. \tag{4.10}$$

For convenience we choose to define the commonly recurring factor

$$\bar{\alpha}_s = \frac{N\alpha_s}{\pi}. \tag{4.11}$$

In the next section we discuss how to calculate the leading (ω-plane) singularity of $f(\omega, \mathbf{k_1}, \mathbf{k_2}, \mathbf{q})$ which determines the leading logarithm contribution to the amplitude $\mathcal{A}^{(1)}(s, t)$.

4.2 The BFKL equation

As discussed above, the leading logarithm contribution to the colour singlet exchange amplitude is given by the infinite sum of ladders in which the vertical lines are reggeized gluons, and the couplings to the horizontal rungs are given by the effective vertices, Γ, of Eq. (3.11), but with a colour factor that projects colour singlet exchange.

One may ask why we only allow reggeized gluons in the vertical lines. Is it not possible that some of the vertical lines are Pomerons themselves, so that we have a similar bootstrap to that which we found in the case of the reggeized gluon? The answer to this goes back to the statement that the Pomeron starts in perturbation theory at one order in α_s higher than the reggeized gluon. The replacement, therefore, of any one of the reggeized gluons in the vertical lines by a Pomeron gives a contribution in any order of perturbation theory which is suppressed by a factor of $\ln s$ and is thus neglected in the leading logarithm approximation.
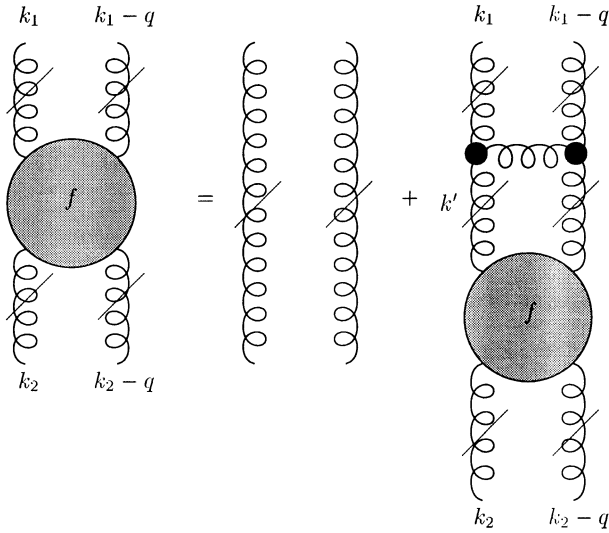
Fig. 4.2. Integral equation for f.

The quantity $f(\omega, \mathbf{k_1}, \mathbf{k_2}, \mathbf{q})$ is therefore given by an integral equation analogous to Eq.(3.46) for the octet quantity $\mathcal{F}^{(8)}(\omega, \mathbf{k}, \mathbf{q})$. However, the addition of an extra rung introduces a colour factor of

$$\frac{\delta_{cd} f_{cae} f_{dbe}}{\delta_{ab}} = N$$

rather than $N/2$ as was the case for colour octet exchange. Once again the Born term is just the exchange of two reggeized gluons and the integral equation equivalent of Eq.(3.46) is shown in Fig. 4.2 and reads

$$(\omega - \epsilon_G(-\mathbf{k_1^2}) - \epsilon_G(-(\mathbf{k_1} - \mathbf{q})^2)) f(\omega, \mathbf{k_1}, \mathbf{k_2}, \mathbf{q})$$
$$= \delta^2(\mathbf{k_1} - \mathbf{k_2}) - \frac{\bar{\alpha}_s}{2\pi} \int d^2 \mathbf{k'} \left[\frac{\mathbf{q}^2}{(\mathbf{k'} - \mathbf{q})^2 \mathbf{k_1^2}} \right.$$
$$\left. - \frac{1}{(\mathbf{k'} - \mathbf{k_1})^2} \left(1 + \frac{(\mathbf{k_1} - \mathbf{q})^2 \mathbf{k'}^2}{(\mathbf{k'} - \mathbf{q})^2 \mathbf{k_1^2}} \right) \right] f(\omega, \mathbf{k'}, \mathbf{k_2}, \mathbf{q}). \qquad (4.12)$$

In the special case of zero momentum transfer, i.e. $\mathbf{q} = 0$, we can simplify this equation to read,

$$[\omega - 2\epsilon_G(-\mathbf{k_1^2})]f(\omega, \mathbf{k_1}, \mathbf{k_2}, \mathbf{0}) = \delta^2(\mathbf{k_1} - \mathbf{k_2})$$
$$+ \bar{\alpha}_s \int \frac{d^2\mathbf{k}'}{\pi} \frac{f(\omega, \mathbf{k}', \mathbf{k_2}, \mathbf{0})}{(\mathbf{k}' - \mathbf{k_1})^2}. \qquad (4.13)$$

Equation (4.12) has a remarkable property – *it is infra-red finite*. In order to see this we use Eqs.(3.48) and (3.49) and exploit the shift of integration variable $\mathbf{k}' \to (\mathbf{k_1} - \mathbf{k}')$ which allows us to make the replacements

$$\frac{1}{\mathbf{k}'^2(\mathbf{k_1} - \mathbf{k}')^2} \to \frac{2}{(\mathbf{k_1} - \mathbf{k}')^2[\mathbf{k}'^2 + (\mathbf{k_1} - \mathbf{k}')^2]} \qquad (4.14)$$

and

$$\frac{1}{(\mathbf{k}' - \mathbf{q})^2(\mathbf{k_1} - \mathbf{k}')^2} = \frac{2}{(\mathbf{k_1} - \mathbf{k}')^2[(\mathbf{k}' - \mathbf{q})^2 + (\mathbf{k_1} - \mathbf{k}')^2]}. \qquad (4.15)$$

Equation (4.12) may then be rewritten:

$$\omega f(\omega, \mathbf{k_1}, \mathbf{k_2}, \mathbf{q}) = \delta^2(\mathbf{k_1} - \mathbf{k_2})$$
$$+ \frac{\bar{\alpha}_s}{2\pi} \int d^2\mathbf{k}' \left[\frac{-\mathbf{q}^2}{(\mathbf{k}' - \mathbf{q})^2\mathbf{k_1^2}} f(\omega, \mathbf{k}', \mathbf{k_2}, \mathbf{q}) \right.$$
$$+ \frac{1}{(\mathbf{k}' - \mathbf{k_1})^2} \left(f(\omega, \mathbf{k}', \mathbf{k_2}, \mathbf{q}) - \frac{\mathbf{k_1^2} f(\omega, \mathbf{k_1}, \mathbf{k_2}, \mathbf{q})}{\mathbf{k}'^2 + (\mathbf{k_1} - \mathbf{k}')^2} \right).$$
$$+ \frac{1}{(\mathbf{k}' - \mathbf{k_1})^2} \left(\frac{(\mathbf{k_1} - \mathbf{q})^2\mathbf{k}'^2 f(\omega, \mathbf{k}', \mathbf{k_2}, \mathbf{q})}{(\mathbf{k}' - \mathbf{q})^2\mathbf{k_1^2}} \right.$$
$$\left. \left. - \frac{(\mathbf{k_1} - \mathbf{q})^2 f(\omega, \mathbf{k_1}, \mathbf{k_2}, \mathbf{q})}{(\mathbf{k}' - \mathbf{q})^2 + (\mathbf{k_1} - \mathbf{k}')^2} \right) \right]. \qquad (4.16)$$

This is the BFKL equation.

The infra-red finiteness can now be seen by observing that the terms in parentheses multiplying the factor $1/(\mathbf{k}' - \mathbf{k_1})^2$ vanish at $\mathbf{k_1} = \mathbf{k}'$. It was in order to make this explicit that the manipulations Eqs.(4.14) and (4.15) were employed. This cancellation justifies our hitherto cavalier treatment of infra-red divergent integrals. This cancellation of infra-red divergences has also been demonstrated by Jaroszewicz (1980) using Ward identities and working in Coulomb gauge.

In fact, the cancellation of the infra-red divergences can be used to justify *a postiori* the use of the strong ordering of the longitudinal components of momenta (i.e. the multi-Regge regime). We have established, in Chapter 2, that the leading logarithm contribution to the integration over longitudinal momenta requires the multi-Regge kinematics. This provides the leading logarithm contribution *provided there are no further logarithms generated by the integration over transverse momenta*. The infra-red finiteness of the BFKL equation means that no such extra logarithms can occur. It is important to appreciate that, in order to ensure the infra-red finiteness, we had to integrate over all intermediate states (of the cut amplitude). It has been pointed out by Marchesini (1995) that for some associated (i.e. not fully inclusive) distributions the infra-red finiteness is lost and consequently the multi-Regge kinematics no longer leads to the leading logarithm contribution. We shall return to this matter at the end of Chapter 6.

4.3 The solution for zero momentum transfer

To keep the mathematics simpler, we first consider the solution to Eq.(4.16) in the case where $\mathbf{q} = 0$ (i.e. we look at the intercept of the QCD Pomeron at $t = 0$). In this case, the BFKL equation becomes

$$\omega f(\omega, \mathbf{k_1}, \mathbf{k_2}, 0) = \delta^2(\mathbf{k_1} - \mathbf{k_2}) + \mathcal{K}_0 \bullet f(\omega, \mathbf{k_1}, \mathbf{k_2}, 0), \quad (4.17)$$

where

$$\mathcal{K}_0 \bullet f(\omega, \mathbf{k_1}, \mathbf{k_2}, 0) = \frac{\bar{\alpha}_s}{\pi} \int \frac{d^2 \mathbf{k'}}{(\mathbf{k_1} - \mathbf{k'})^2}$$

$$\times \left[f(\omega, \mathbf{k'}, \mathbf{k_2}, 0) - \frac{\mathbf{k}_1^2}{[\mathbf{k'}^2 + (\mathbf{k_1} - \mathbf{k'})^2]} f(\omega, \mathbf{k_1}, \mathbf{k_2}, 0) \right]. \quad (4.18)$$

This is a Green function equation which is solved if we can find the complete set of eigenfunctions, $\phi_i(\mathbf{k})$ (with eigenvalues λ_i), of the integral operator (or **kernel**), $\mathcal{K}_0$, i.e.

$$\mathcal{K}_0 \bullet \phi_i(\mathbf{k}) = \lambda_i \phi_i(\mathbf{k}).$$

The eigenfunctions must obey the completeness relation

$$\sum_i \phi_i(\mathbf{k_1}) \phi_i^*(\mathbf{k_2}) = \delta^2(\mathbf{k_1} - \mathbf{k_2}),$$

where the sum over the eigenfunction label, i, may involve an integral over a continuous variable. The solution to the Green function equation is then given by

$$f(\omega, \mathbf{k_1}, \mathbf{k_2}, 0) = \sum_i \frac{\phi_i(\mathbf{k_1})\phi_i^*(\mathbf{k_2})}{\omega - \lambda_i}. \qquad (4.19)$$

Since $\mathbf{k}$ is a vector in the two-dimensional transverse space we can write

$$\mathbf{k} = (k, \theta)$$
$$\mathbf{k}' = (k', \theta')$$

and

$$d^2\mathbf{k}' = \frac{1}{2}dk'^2 d\theta'.$$

By Fourier analysis $\phi_i(\mathbf{k})$ can be expanded in powers of $\exp(i\theta)$ with coefficients $\phi_i^n(k)$

$$\phi_i(\mathbf{k}) = \sum_{n=0}^{\infty} \phi_i^n(k)\frac{e^{in\theta}}{\sqrt{2\pi}}.$$

Inserting each of these components into $\mathcal{K}_0 \bullet \phi_i$ and performing the angular integral over θ' gives

$$\mathcal{K}_0 \bullet \phi_i^n(k) = \bar{\alpha}_s e^{in\theta} \int dk'^2 \left\{ \frac{1}{|k'^2 - k^2|} \right.$$
$$\times \left[\left(\frac{k'k}{\max(k^2, k'^2)} \right)^n \phi_i^n(k') - \frac{k^2}{\max(k^2, k'^2)}\phi_i^n(k) \right]$$
$$\left. + \frac{4\phi_i^n(k)}{\sqrt{4k'^4 + k^4}} \left[\frac{k'^2\theta(k^2 - k'^2)}{k^2 + \sqrt{4k'^4 + k^4}} - \theta(k'^2 - k^2)\frac{k^2}{k'^2} \right] \right\}. \qquad (4.20)$$

After the integral over k'^2 the last two terms cancel each other, in anticipation of which we rewrite the right hand side of Eq.(4.20) as

$$\bar{\alpha}_s e^{in\theta} \int_0^{k^2} \frac{dk'^2}{k^2 - k'^2} \left[\left(\frac{k'}{k} \right)^n \phi_i^n(k') - \phi_i^n(k) \right]$$
$$+ \bar{\alpha}_s e^{in\theta} \int_{k^2}^{\infty} \frac{dk'^2}{k'^2 - k^2} \left[\left(\frac{k}{k'} \right)^n \phi_i^n(k') - \frac{k^2}{k'^2}\phi_i^n(k) \right]. \qquad (4.21)$$

Now since there is no infra-red divergence (i.e. no need to introduce a dimensionful scale to regularize the integrals in Eq.(4.21)) and since the kernel is a dimensionless operator, it follows that

$\phi_i^n(k)$ behaves like a power of k^2. In order to have a set of eigenfunctions that obey the completeness relation we need to restrict this power behaviour to the form

$$\phi_\nu(k) \sim (k^2)^{-1/2+i\nu}, \qquad (4.22)$$

where $-\infty < \nu < \infty$. Thus the complete eigenfunctions are

$$\phi_\nu^n(\mathbf{k}) = \frac{1}{\pi\sqrt{2}}(k^2)^{-1/2+i\nu}e^{in\theta}. \qquad (4.23)$$

These are normalized so as to satisfy

$$\int d^2\mathbf{k}\phi_\nu^n(\mathbf{k})\phi_{\nu'}^{n'*}(\mathbf{k}) = \delta(\nu - \nu')\delta(n - n'). \qquad (4.24)$$

To find the eigenvalues we insert the function $\phi_\nu^n(\mathbf{k})$ into Eq.(4.21) and obtain

$$e^{in\theta}\phi_\nu^n(\mathbf{k})\bar{\alpha}_s\left[\int_0^1 dz\frac{(z^{(n-1)/2+i\nu} - 1)}{(1 - z)} + \int_0^1 dw\frac{(w^{(n-1)/2-i\nu} - 1)}{(1 - w)}\right],$$

where

$$z = \frac{k'^2}{k^2} \quad \text{and} \quad w = \frac{k^2}{k'^2}.$$

Hence the eigenvalue, $\omega_n(\nu)$, is

$$\omega_n(\nu) = \bar{\alpha}_s\chi_n(\nu), \qquad (4.25)$$

where

$$\chi_n(\nu) = 2\int_0^1 dz\frac{z^{(n-1)/2}\cos(\nu\ln z) - 1}{(1 - z)}. \qquad (4.26)$$

This is a standard integral which is given in terms of the digamma function, ψ (the logarithmic derivative of the Γ function), i.e.

$$\chi_n(\nu) = 2\left(-\gamma_E - \Re e\left[\psi\left((n + 1)/2 + i\nu\right)\right]\right), \qquad (4.27)$$

where $\gamma_E \approx 0.577$ is Euler's constant.

Thus the solution for $f(\omega, \mathbf{k_1}, \mathbf{k_2}, \mathbf{0})$ is

$$f(\omega, \mathbf{k_1}, \mathbf{k_2}, \mathbf{0}) = \sum_{n=0}^{\infty}\int_{-\infty}^{\infty}d\nu\left(\frac{k_1^2}{k_2^2}\right)^{i\nu}\frac{e^{in(\theta_1 - \theta_2)}}{2\pi^2 k_1 k_2}\frac{1}{(\omega - \bar{\alpha}_s\chi_n(\nu))}. \qquad (4.28)$$

Our first observation is that since ν is a continuous variable we do not obtain an isolated pole in the Mellin transform which we can associate with the intercept of the Pomeron. Leading logarithm perturbation theory gives us a cut rather than a pole. We shall return to this matter later.

We are interested in the leading $\ln s$ behaviour which means the singularity with the largest real part in the ω-plane. This allows us to make a number of simplifications. Since the function $\chi_n(\nu)$ decreases with increasing n, we are at liberty to restrict the sum over n in Eq.(4.28) to the case where $n = 0$. Furthermore, $\chi_0(\nu)$ decreases with increasing $|\nu|$ so we can expand $\chi_0(\nu)$ as a power series in ν and keep only the first two terms. We obtain

$$\chi_0(\nu) = 4\ln 2 - 14\zeta(3)\nu^2 + \cdots, \tag{4.29}$$

with $\zeta(3) = \sum_r (1/r^3) \approx 1.202$. In this approximation

$$f(\omega, \mathbf{k_1}, \mathbf{k_2}, 0) \approx \frac{1}{\pi k_1 k_2} \int_{-\infty}^{\infty} \frac{d\nu}{2\pi} \left(\frac{k_1^2}{k_2^2}\right)^{i\nu} \frac{1}{(\omega - \omega_0 + a^2\nu^2)}, \tag{4.30}$$

with

$$\omega_0 = 4\bar{\alpha}_s \ln 2 \tag{4.31}$$

being the position of the leading singularity (the branch point of the cut) and

$$a^2 = 14\bar{\alpha}_s\zeta(3). \tag{4.32}$$

We can perform the integration over ν (using contour integration) and obtain

$$f(\omega, \mathbf{k_1}, \mathbf{k_2}, 0) \approx \frac{1}{2\pi a k_1 k_2} \left(\frac{k_1 k_2}{\max(k_1^2, k_2^2)}\right)^{\sqrt{\omega - \omega_0}/a} \frac{1}{\sqrt{\omega - \omega_0}}. \tag{4.33}$$

Moreover, one can invert the Mellin transform to expose the s-dependence of the colour singlet amplitude. This is most easily effected by inverting Eq.(4.30) before integrating over ν. We find

$$F(s, \mathbf{k_1}, \mathbf{k_2}, 0) \approx \frac{1}{\sqrt{\mathbf{k_1^2 k_2^2}}} \left(\frac{s}{\mathbf{k}^2}\right)^{\omega_0} \frac{1}{\sqrt{\pi \ln(s/\mathbf{k}^2)}}$$
$$\times \frac{1}{2\pi a} \exp\left(-\frac{\ln^2(\mathbf{k_1^2}/\mathbf{k_2^2})}{4a^2 \ln(s/\mathbf{k}^2)}\right). \tag{4.34}$$

This is the inverse transform of Eq.(4.33), i.e. the full amplitude for quark–quark forward elastic scattering is simply (see Eq.(4.7))

$$\frac{\mathcal{A}^{(1)}(s, 0)}{s} = 4i\alpha_s^2 \delta_{\lambda_1'\lambda_1} \delta_{\lambda_2'\lambda_2} G_0^{(1)} \int \frac{d^2\mathbf{k_1}}{\mathbf{k_1^2}} \frac{d^2\mathbf{k_2}}{\mathbf{k_2^2}} F(s, \mathbf{k_1}, \mathbf{k_2}, 0). \tag{4.35}$$

Note the factor of $1/\sqrt{\ln s}$. It arises from the fact that the Mellin transform contains an ω-plane cut rather than a simple pole.

The effect of including higher order terms in the expansion of $\chi_0(\nu)$ is to add terms which are suppressed by powers of $\ln s$, and so we are formally justified in neglecting them.

4.4 Impact factors

Before we move on to the somewhat more complicated problem of solving the BFKL equation for non-zero momentum transfer, we digress a little to discuss the matter of impact factors.

So far we have considered only quark–quark elastic scattering, where the external quarks are on shell. In practice, this is not what actually happens: the Pomeron couples to a hadron inside which the partons are slightly off-shell. Indeed, in the case of quark–quark scattering, despite the fact that $f(\omega, \mathbf{k_1}, \mathbf{k_2}, \mathbf{q})$ does not contain any infra-red singularities, the amplitude nevertheless diverges owing to the remaining integrals over $\mathbf{k_1}$ and $\mathbf{k_2}$ which develop infra-red singularities when $\mathbf{k_1}$ or $\mathbf{k_2}$ go to zero (or when $(\mathbf{k_1} - \mathbf{q})$ or $(\mathbf{k_2} - \mathbf{q})$ go to zero). These infra-red divergences are regulated by the slight off-shellness of the quarks (or gluons) to which the QCD Pomeron couples inside the hadron.

This leads us to introduce the quantity Φ, which is called the **impact factor** and accounts for the coupling of the Pomeron to the hadrons. We will consider here the case of elastic hadron–hadron scattering.

For elastic scattering of a hadron with initial momentum p_1 and a hadron with initial momentum p_2 (and final momenta $p_1 - q$ and $p_2 + q$ respectively), the Mellin transform of the scattering amplitude is given by (see Fig. 4.3)[†]

$$\mathcal{A}^{(1)}(\omega, t) = \frac{\mathcal{G}}{(2\pi)^4} \int d^2\mathbf{k_1} d^2\mathbf{k_2} \frac{\Phi_1(\mathbf{k_1}, \mathbf{q})\Phi_2(\mathbf{k_2}, \mathbf{q})}{\mathbf{k_2^2}(\mathbf{k_1} - \mathbf{q})^2} f(\omega, \mathbf{k_1}, \mathbf{k_2}, \mathbf{q}),$$

(4.36)

where Φ_1 and Φ_2 are the impact factors associated with the two scattering hadrons. The factor, $\mathcal{G}$, is the colour factor for the process.

[†] Note that $\mathcal{A}^{(1)}(\omega, t)$ is the Mellin transform of $\Im m \mathcal{A}^{(1)}(s, t)/s$ as defined in Eq. (4.7).
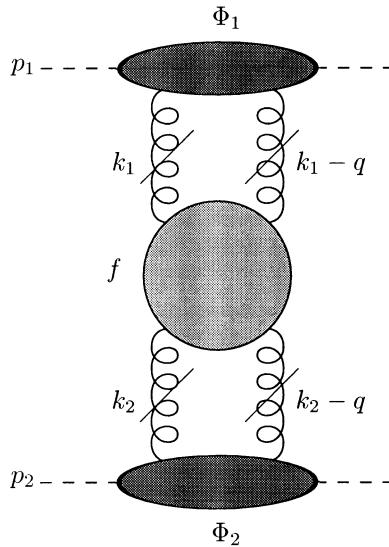
Fig. 4.3. Pomeron coupling to hadrons.

With these definitions, for the process of quark–quark elastic scattering the colour factor is

$$\mathcal{G} = G_0^{(1)}$$

and the impact factor is

$$\Phi_q = 2\pi g^2 \delta_{\lambda\lambda'}. \tag{4.37}$$

In order to calculate the impact factors we would need to know a great deal of detail about the wavefunction of the partons inside the hadron. Since this information is generally not available, models have to be used to calculate these impact factors. We will take a very simple model, namely, we consider meson–meson scattering and assume that the quarks are scalar particles and that the meson couples to quarks via a point-like coupling with dimensionful coupling constant, h. This last simplification just means that we do not have to worry about taking traces of Dirac matrices, and simplifies the expression that we obtain, but it does not qualitatively alter the result (the more physical case of spin-$\frac{1}{2}$ quarks coupling to vector photons is examined in the appendix to Chapter 6). In order to regulate the infra-red divergences we will
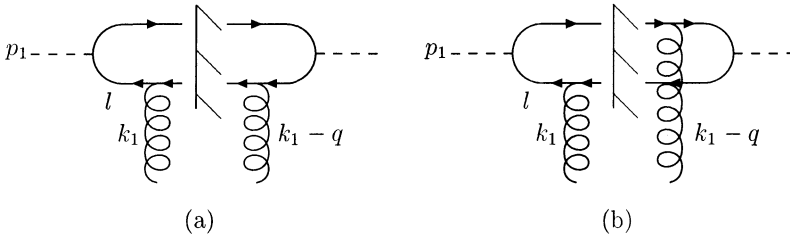
Fig. 4.4. Graphs for calculating impact factors.

have to introduce a quark mass, m, but we shall assume that the mesons remain massless.

The diagrams contributing to Φ_1 are shown in Fig. 4.4. We only need to calculate the leading order contribution since all higher order corrections are included in the quantity $f(\omega, \mathbf{k_1}, \mathbf{k_2}, \mathbf{q})$. Since we are using dispersive techniques to calculate the imaginary part of the amplitude (recall that the Pomeron amplitude is purely imaginary in the leading logarithm approximation) we consider the cut diagrams shown.

The momenta in the diagrams of Fig. 4.4 are labelled in such a way that the cut lines have momenta $l - k_1$ and $p_1 - l$ and so the two-body phase space may be written

$$d(P.S.^2) = \int \frac{d^4k_1}{(2\pi)^3} \frac{d^4l}{(2\pi)^3} \delta((k_1 - l)^2 - m^2) \delta((p_1 - l)^2 - m^2).$$

The diagram Fig. 4.4(a) leads to the amplitude,

$$A_{(a)}^{\mu\nu} = 4\pi\alpha_s h^2 \frac{(2l - k_1)^\mu (2l - k_1 - q)^\nu}{(l^2 - m^2)((l - q)^2 - m^2)}, \qquad (4.38)$$

whereas the diagram of Fig. 4.4(b) gives

$$A_{(b)}^{\mu\nu} = 4\pi\alpha_s h^2 \frac{(2l - k_1)^\mu (2l - 2p_1 - k_1 + q)^\nu}{(l^2 - m^2)((l - p_1 - k_1 + q)^2 - m^2)}. \qquad (4.39)$$

We have suppressed the colour matrices since they lead to the final colour factor of $\mathcal{G} = N^2 G_0^{(1)}$ (the factor N^2 arises because we no longer average over the incident quark colours).

As usual, we introduce Sudakov variables for l and k_1, i.e.

$$l^\mu = \rho p_1^\mu + \lambda p_2^\mu + l_\perp^\mu$$
$$k_1^\mu = \rho_1 p_1^\mu + \lambda_1 p_2^\mu + k_{1\perp}^\mu.$$

Recall that we are working in the eikonal approximation for which $\rho_1 \ll 1$ and so we are only interested in terms which are proportional to $p_1^\mu p_1^\nu$ in the numerator. The numerators then simplify to $4\rho^2 p_1^\mu p_1^\nu$ for Fig. 4.4(a) and $-4\rho(1-\rho)p_1^\mu p_1^\nu$ for Fig. 4.4(b). The limits on ρ are actually $\rho_1 < \rho < 1$, but since $\rho_1 \ll 1$ we can neglect ρ_1 compared with ρ up to corrections of order $\mathbf{k}_1^2/s$, $\mathbf{q}^2/s$.

In terms of the Sudakov variables the phase-space integral then becomes

$$d(P.S.^2) = \frac{1}{(2\pi)^6}\frac{1}{4}\int d\rho\, d\rho_1 d\lambda d\lambda_1 d^2\mathbf{l}\, d^2\mathbf{k_1}$$
$$\times\ \delta((1-\rho)\lambda + \mathbf{l}^2/s + m^2/s)\delta(\rho(\lambda-\lambda_1) - (\mathbf{l} - \mathbf{k}_1)^2/s + m^2/s).$$

After using the delta functions to fix λ and λ_1, and the on-shell condition for the final state mesons, $2p_1.q = -\mathbf{q}^2$, we find

$$A_{(a)}^{\mu\nu} = \frac{4\pi\alpha_s h^2\ 4\rho^2(1-\rho)^2\ p_1^\mu p_1^\nu}{(\mathbf{l}^2+m^2)(\mathbf{l}^2+\mathbf{q}^2(1-\rho)^2 - 2\mathbf{q}\cdot\mathbf{l}(1-\rho)+m^2)} \qquad (4.40)$$

and

$$A_{(b)}^{\mu\nu} = -\frac{4\pi\alpha_s h^2\ 4\rho^2(1-\rho)^2\ p_1^\mu p_1^\nu}{(\mathbf{l}^2+m^2)((\mathbf{l}-\mathbf{k_1})^2 + 2\rho\mathbf{q}\cdot(\mathbf{l}-\mathbf{k_1})+\mathbf{q}^2\rho^2+m^2)}. \qquad (4.41)$$

We now turn to the integral over the phase space. The integration over the transverse momentum $\mathbf{l}$ is most easily effected by introducing a Feynman parameter, τ, to combine the denominators, i.e. we use

$$\frac{1}{AB} = \int_0^1 d\tau \frac{1}{[A + \tau(B-A)]^2}. \qquad (4.42)$$

Thus we find that,

$$2\int d(P.S.^2)(A_{(a)}^{\mu\nu} + A_{(b)}^{\mu\nu})$$

$$= \frac{\alpha_s h^2}{(2\pi)^4}2p_1^\mu p_1^\nu \int d\rho\, d\rho_1\, d^2\mathbf{k_1}\, d\tau\, \rho(1-\rho)$$

$$\times\ \left[\frac{1}{(\mathbf{q}^2\rho^2\tau(1-\tau)+m^2)} - \frac{1}{[(\mathbf{k_1}-\rho\mathbf{q})^2\tau(1-\tau)+m^2]}\right] \qquad (4.43)$$

and we have multiplied by 2 to include the related graphs in which the gluons couple to the opposite quark lines from those shown in Fig. 4.4. Note that the contribution from Fig. 4.4(a) is minus the contribution from Fig. 4.4(b) with $\mathbf{k_1}$ set to zero. The minus sign can be understood from the fact that in Fig. 4.4(a) the

gluon on the right of the cut couples to the antiquark whilst in Fig. 4.4(b) it couples to a quark. This guarantees the vanishing of the impact factor Φ_1 when $\mathbf{k_1} = 0$, thereby regularizing the remaining infra-red divergence arising from the integration over $\mathbf{k_1}$. The infra-red finiteness of the colour singlet exchange amplitude can be interpreted as the cancellation between divergences arising from soft virtual gluon corrections (which are associated with the reggeization of the gluons in the vertical lines of the ladder as explained in the preceding chapter) and gluon bremsstrahlung (associated with adding more rungs to the ladder). The cancellation occurs for colour singlet amplitudes in accordance with the Kinoshita (1962), Lee, Nauenberg (1964) theorem. This theorem was originally derived for the case of QED. For non-abelian gauge theories it also works when applied to processes with colour singlet external states but *not* for colour non-singlet exchange amplitudes. That is why the Pomeron exchange amplitude is infra-red finite but the reggeized gluon is not.

There is a corresponding factor to that of Eq.(4.43) arising from the lower meson–Pomeron vertex (obtained by making the replacement $\mathbf{k_1} \rightarrow \mathbf{k_2}$ and integrating over λ_2 rather than ρ_1). Each of these factors must then be contracted into the four-gluon Green function. From Eq.(4.8), which relates $f(\omega, \mathbf{k_1}, \mathbf{k_2}, \mathbf{q})$ to the Green function, and Eq.(4.36), which defines the impact factors in terms of $f(\omega, \mathbf{k_1}, \mathbf{k_2}, \mathbf{q})$, we then find

$$\Phi_1(\mathbf{k_1}, \mathbf{q}) = \alpha_s h^2 \int d\rho \, d\tau \, \rho(1-\rho) \left[\frac{1}{(\mathbf{q}^2 \rho^2 \tau(1-\tau) + m^2)} - \frac{1}{[(\mathbf{k_1} - \rho\mathbf{q})^2 \tau(1-\tau) + m^2]} \right]. (4.44)$$

The expression for $\Phi_2(\mathbf{k_2}, \mathbf{q})$ is obtained *mutatis mutandis*.

For zero momentum transfer the expression for the impact factors simplifies to

$$\Phi_1(\mathbf{k_1}, \mathbf{0}) = \frac{\alpha_s h^2}{6} \int d\tau \frac{\mathbf{k_1}^2 \tau(1-\tau)}{m^2(\mathbf{k_1}^2 \tau(1-\tau) + m^2)}, \qquad (4.45)$$

with a similar expression for $\Phi_2(\mathbf{k_2}, \mathbf{0})$.

Following Balitsky & Lipatov (1978) we have organized the perturbation expansion in such a way that we consider only the leading order contribution to the impact factors and in particular we describe the meson in terms of its lowest order Fock space

component (i.e. a quark and an antiquark), all higher order terms being in the quantity $f(\omega, \mathbf{k_1}, \mathbf{k_2}, \mathbf{q})$. This is a matter of choice and we could have organized the perturbation expansion differently. Indeed Mueller (1994), Chen & Mueller (1995), Nikolaev & Zakharov (1994) and Nikolaev, Zakharov & Zoller (1994a, 1994b) have considered the Fock space expansion of a heavy quark meson, starting with a quark–antiquark pair and adding any number of soft gluons. From this procedure an expression for the soft gluon contribution to the meson wavefunction can be obtained and this in turn leads to a determination of the low-x structure function of the meson which is shown to obey the BFKL equation. We shall have more to say on this way of looking at high energy scattering in Chapter 8.

A derivation of structure functions from the consideration of the sum of all possible soft gluon insertions has also been carried out by Catani, Fiorani & Marchesini (1990a,b), Catani, Fiorani, Marchesini & Oriani (1991) and Ciafaloni (1988). The application of the $t = 0$ BFKL equation in low-x deep inelastic scattering will be discussed in detail in Chapter 6.

4.5 Solution for non-zero momentum transfer

The solution of the BFKL equation for t $(= -\mathbf{q}^2)$ not equal to zero proved rather recalcitrant. Eight years elapsed from the publication of the paper by Balitsky & Lipatov (1978), in which the solution for zero momentum transfer was presented, until Lipatov (1986) solved the equation for non-zero momentum transfer. In order to do so it was first necessary to perform a two-dimensional Fourier transform to express the amplitude $f(\omega, \cdots)$ not in terms of transverse momenta $\mathbf{k_1}, \mathbf{k_2}, \mathbf{q} - \mathbf{k_1}, \mathbf{q} - \mathbf{k_2}$, but in terms of corresponding impact parameters $\mathbf{b_1}, \mathbf{b_2}, \mathbf{b_1'}, \mathbf{b_2'}$. Thus we define

$$\tilde{f}(\omega, \mathbf{b_1}, \mathbf{b_1'}, \mathbf{b_2}, \mathbf{b_2'}) = \int d^2\mathbf{k_1} d^2\mathbf{k_2} d^2\mathbf{q}$$

$$\times \left[e^{i(\mathbf{k_1}\cdot\mathbf{b_1} + (\mathbf{q}-\mathbf{k_1})\cdot\mathbf{b_1'} - \mathbf{k_2}\cdot\mathbf{b_2} - (\mathbf{q}-\mathbf{k_2})\cdot\mathbf{b_2'})} \frac{f(\omega, \mathbf{k_1}, \mathbf{k_2}, \mathbf{q})}{\mathbf{k_2^2}(\mathbf{k_1} - \mathbf{q})^2} \right] \quad (4.46)$$

and the BFKL equation in impact parameter space becomes

$$\omega \partial^2_{\mathbf{b_1}} \partial^2_{\mathbf{b'_1}} \tilde{f}(\omega, \mathbf{b_1}, \mathbf{b'_1}, \mathbf{b_2}, \mathbf{b'_2}) \ = \ (2\pi)^4 \delta^2(\mathbf{b_1} - \mathbf{b_2}) \delta^2(\mathbf{b'_1} - \mathbf{b'_2})$$

$$+ \frac{\bar{\alpha}_s}{2\pi} \Bigg\{ (2\pi)^2 \delta^2(\mathbf{b_1} - \mathbf{b'_1})(\partial_{\mathbf{b_1}} + \partial_{\mathbf{b'_1}})^2 \tilde{f}(\omega, \mathbf{b_1}, \mathbf{b'_1}, \mathbf{b_2}, \mathbf{b'_2})$$

$$+ \partial^2_{\mathbf{b_1}} \int \frac{d^2\mathbf{c}}{(\mathbf{b_1} - \mathbf{c})^2} \Bigg[\partial^2_{\mathbf{b'_1}} \tilde{f}(\omega, \mathbf{c}, \mathbf{b'_1}, \mathbf{b_2}, \mathbf{b'_2})$$

$$- \frac{(\mathbf{b_1} - \mathbf{b'_1})^2}{\Big[(\mathbf{b_1} - \mathbf{c})^2 + (\mathbf{b'_1} - \mathbf{c})^2 \Big]} \partial^2_{\mathbf{b'_1}} \tilde{f}(\omega, \mathbf{b_1}, \mathbf{b'_1}, \mathbf{b_2}, \mathbf{b'_2}) \Bigg]$$

$$+ \partial^2_{\mathbf{b'_1}} \int \frac{d^2\mathbf{c}}{(\mathbf{b'_1} - \mathbf{c})^2} \Bigg[\partial^2_{\mathbf{b_1}} \tilde{f}(\omega, \mathbf{b_1}, \mathbf{c}, \mathbf{b_2}, \mathbf{b'_2})$$

$$- \frac{(\mathbf{b_1} - \mathbf{b'_1})^2}{\Big[(\mathbf{b_1} - \mathbf{c})^2 + (\mathbf{b'_1} - \mathbf{c})^2 \Big]} \partial^2_{\mathbf{b_1}} \tilde{f}(\omega, \mathbf{b_1}, \mathbf{b'_1}, \mathbf{b_2}, \mathbf{b'_2}) \Bigg] \Bigg\}, \quad (4.47)$$

where $\partial^2_{\mathbf{b}}$ is the two-dimensional d'Alembertian operator with respect to the impact parameter $\mathbf{b}$. We explain how this equation is derived in the appendix to this chapter.

Once again this is a Green function equation and can be solved if we can find a complete set of eigenfunctions, $\tilde{\phi}_i(\mathbf{b}, \mathbf{b'})$, of the kernel $\tilde{\mathcal{K}}_0$, where

$$\tilde{\mathcal{K}}_0 \bullet \tilde{\phi}_i(\mathbf{b}, \mathbf{b'}) \ = \ \frac{\bar{\alpha}_s}{2\pi} \Bigg\{ \partial^2_{\mathbf{b}} \int \frac{d^2\mathbf{c}}{(\mathbf{b} - \mathbf{c})^2} \Bigg[\partial^2_{\mathbf{b'}} \tilde{\phi}_i(\mathbf{c}, \mathbf{b'})$$

$$- \frac{(\mathbf{b} - \mathbf{b'})^2}{\Big[(\mathbf{b} - \mathbf{c})^2 + (\mathbf{b'} - \mathbf{c})^2 \Big]} \partial^2_{\mathbf{b'}} \tilde{\phi}_i(\mathbf{b}, \mathbf{b'}) \Bigg]$$

$$+ \partial^2_{\mathbf{b'}} \int \frac{d^2\mathbf{c}}{(\mathbf{b'} - \mathbf{c})^2} \Bigg[\partial^2_{\mathbf{b}} \tilde{\phi}_i(\mathbf{b}, \mathbf{c})$$

$$- \frac{(\mathbf{b} - \mathbf{b'})^2}{\Big[(\mathbf{b} - \mathbf{c})^2 + (\mathbf{b'} - \mathbf{c})^2 \Big]} \partial^2_{\mathbf{b}} \tilde{\phi}_i(\mathbf{b}, \mathbf{b'}) \Bigg] \Bigg\} \quad (4.48)$$

(for $\mathbf{b} \neq \mathbf{b'}$).

These eigenfunctions are best described by expressing the two-dimensional vectors $\mathbf{b_i} = (b_i, \theta_i)$ in terms of complex numbers, namely,

$$b_i = b_i e^{i\theta_i},$$

so that $\partial_{\mathbf{b_i}}^2 = 4\partial^2/\partial b_i \partial b_i^*$. The eigenfunctions of $\tilde{\mathcal{K}}_0$ are then given by

$$\tilde{\phi}_n^\nu(b, b', c) = \left(\frac{(b - b')}{(b - c)(b' - c)}\right)^n \left(\frac{|b - b'|}{|b - c||b' - c|}\right)^{1 + 2i\nu - n}$$

(4.49)

for any two-dimensional (transverse) vector $\mathbf{c}$.

These eigenfunctions were originally identified by exploiting the two-dimensional conformal invariance of Eq.(4.48) and the fact that the expression on the right hand side of Eq.(4.49) is a representation of the two-dimensional conformal group. We shall not concern ourselves with such technicalities in this book.

If the eigenfunctions are inserted into Eq.(4.48), then, after some straightforward but tedious algebra, it can be shown that they are indeed eigenfunctions of $\tilde{\mathcal{K}}_0$ with exactly the same eigenvalues as for the $\mathbf{q}^2 = 0$ case. In other words, the eigenvalues are also given by Eq.(4.25).

The eigenfunctions $\tilde{\phi}_n^\nu$ can be shown to obey the following completeness relation (returning to two-dimensional vector notation):

$$\sum_{n=-\infty}^{\infty} \int_{-\infty}^{\infty} d\nu \int d^2\mathbf{c}(4\nu^2 + n^2)\tilde{\phi}_n^\nu(\mathbf{b_1}, \mathbf{b_1'}, \mathbf{c})\tilde{\phi}_n^{\nu*}(\mathbf{b_2}, \mathbf{b_2'}, \mathbf{c})$$

$$= \frac{1}{4}(2\pi)^4(\mathbf{b_1} - \mathbf{b_1'})^4 \delta^2(\mathbf{b_1} - \mathbf{b_2})\delta^2(\mathbf{b_1'} - \mathbf{b_2'}). \quad (4.50)$$

The derivation of this completeness relation is given in the paper by Lipatov (1986) and we refer the reader to that paper for details. We can also show quite easily that

$$\partial_{\mathbf{b_1}}^2 \partial_{\mathbf{b_1'}}^2 \tilde{\phi}_n^\nu(\mathbf{b_1}, \mathbf{b_1'}, \mathbf{c}) = \frac{\left(4\nu^2 + 1 - n^2\right)^2 + 16n^2\nu^2}{(\mathbf{b_1} - \mathbf{b_1'})^4}\tilde{\phi}_n^\nu(\mathbf{b_1}, \mathbf{b_1'}, \mathbf{c}),$$

(4.51)

which is useful since the operator $\partial_{\mathbf{b_1}}^2 \partial_{\mathbf{b_1'}}^2$ appears on the left hand side of Eq.(4.47).

Combining Eqs.(4.50) and (4.51) we obtain the general solution of Eq.(4.47):

$$\tilde{f}(\omega, \mathbf{b_1}, \mathbf{b_1'}, \mathbf{b_2}, \mathbf{b_2'}) = \sum_{n=-\infty}^{\infty} \int_{-\infty}^{\infty} d\nu \int d^2\mathbf{c}$$

$$\times \frac{(16\nu^2 + 4n^2)}{((4\nu^2 + 1 - n^2)^2 + 16n^2\nu^2)} \frac{\tilde{\phi}_n^\nu(\mathbf{b_1}, \mathbf{b_1'}, \mathbf{c})\tilde{\phi}_n^{\nu*}(\mathbf{b_2}, \mathbf{b_2'}, \mathbf{c})}{(\omega - \bar{\alpha}_s\chi_n(\nu))}. \quad (4.52)$$

Note that for the case where $n = \pm 1$ the integral over ν is interpreted in the sense of its principal value, namely,

$$\int_{-\infty}^{\infty} \frac{d\nu}{\nu^2} f(\nu) = \lim_{\epsilon \to 0} \left[\int_{-\infty}^{-\epsilon} \frac{d\nu}{\nu^2} f(\nu) + \int_{\epsilon}^{\infty} \frac{d\nu}{\nu^2} f(\nu) - 2 \frac{f(0)}{\epsilon} \right].$$

As in the case of zero momentum transfer we look for the leading singularity in ω by considering only the $n = 0$ term in the sum over n and expanding $\chi_0(\nu)$ up to quadratic order in ν. The integration over ν can then be performed. The result is rather cumbersome and we do not write it down here.

There is an important complication that arises if we wish to consider the coupling of the Pomeron to individual quarks inside the hadron. Since Eq.(4.47) is not an equation for $\tilde{f}$ but for $\partial^2_{\mathbf{b_1}} \partial^2_{\mathbf{b'_1}} \tilde{f}$, the solution we have obtained is ambiguous up to the addition of any function which is independent of *one* of $\mathbf{b_1}, \mathbf{b'_1}$ (and by symmetry any function which is independent of *one* of $\mathbf{b_2}, \mathbf{b'_2}$). In transverse momentum space, such terms give rise to ambiguities proportional to $\delta^2(\mathbf{k_1})$ or $\delta^2(\mathbf{k_1} - \mathbf{q})$ (and likewise $\mathbf{k_1} \leftrightarrow \mathbf{k_2}$). These ambiguities are therefore irrelevant when we make a convolution of $f(\omega, \mathbf{k_1}, \mathbf{k_2}, \mathbf{q})$ with impact factors that vanish when any of these transverse momenta vanish.

On the other hand the Born diagram (exchange of two gluons) in impact parameter space should give a contribution to $\tilde{f}(\omega, \mathbf{b_1}, \mathbf{b'_1}, \mathbf{b_2}, \mathbf{b'_2})$ of

$$\tilde{f}(\omega, \mathbf{b_1}, \mathbf{b'_1}, \mathbf{b_2}, \mathbf{b'_2})_{\text{Born}} = \frac{\pi^2}{\omega} \ln \left((\mathbf{b_1} - \mathbf{b_2})^2 \right) \ln \left((\mathbf{b'_1} - \mathbf{b'_2})^2 \right),$$

$$(4.53)$$

whereas Eq.(4.52) in the limit $\alpha_s \to 0$ gives

$$\tilde{f}(\omega, \mathbf{b_1}, \mathbf{b'_1}, \mathbf{b_2}, \mathbf{b'_2})_{\alpha_s \to 0} = \frac{\pi^2}{\omega} \ln \left(\frac{(\mathbf{b_1} - \mathbf{b_2})^2 (\mathbf{b'_1} - \mathbf{b'_2})^2}{(\mathbf{b_1} - \mathbf{b'_2})^2 (\mathbf{b'_1} - \mathbf{b_2})^2} \right)$$

$$\times \ln \left(\frac{(\mathbf{b_1} - \mathbf{b_2})^2 (\mathbf{b'_1} - \mathbf{b'_2})^2}{(\mathbf{b_1} - \mathbf{b'_1})^2 (\mathbf{b_2} - \mathbf{b'_2})^2} \right) . \quad (4.54)$$

We note that Eqs.(4.53) and (4.54) differ by terms which are independent of at least one of $\mathbf{b_1}, \mathbf{b'_1}, \mathbf{b_2}, \mathbf{b'_2}$.

Mueller & Tang (1992) have pointed out that the difference between Eqs.(4.53) and (4.54) can be accounted for by replacing

$\tilde{\phi}_0^\nu(\mathbf{b}, \mathbf{b}', \mathbf{c})$ (Eq.(4.49)) by

$$\tilde{\phi}_0^\nu(\mathbf{b}, \mathbf{b}', \mathbf{c}) = \left(\frac{(\mathbf{b} - \mathbf{b}')^2}{(\mathbf{b} - \mathbf{c})^2 (\mathbf{b}' - \mathbf{c})^2} \right)^{1/2 + i\nu} - \left(\frac{1}{(\mathbf{b} - \mathbf{c})^2} \right)^{1/2 + i\nu}$$
$$- \left(\frac{1}{(\mathbf{b}' - \mathbf{c})^2} \right)^{1/2 + i\nu}. \qquad (4.55)$$

This replacement has no effect on amplitudes obtained by convolution with impact factors which vanish at zero transverse momentum, but they *do* affect the coupling of the Pomeron to individual quarks and hence are important in discussing certain diffractive dissociation processes. This has been considered in detail by Bartels *et al.* (1995) and Forshaw & Ryskin (1995).

We defer further studies of the properties of the non-forward amplitude until Chapter 7.

4.6 Deviations from 'soft' Pomeron behaviour

We have derived the hard Pomeron in (leading logarithm) perturbative QCD. It is quite distinct from the soft Pomeron of Chapter 1. Let us summarize the main differences:

1. The leading singularity of the Mellin transform is a cut and not an isolated pole. We shall return to this matter in the next chapter.

2. The position of the leading singularity gives an s-dependence $s^{\alpha_P(t)}$, where

$$\alpha_P(t) = 1 + 4\bar{\alpha}_s \ln 2.$$

This is typically much larger than the phenomenologically observed intercept of the Pomeron at $\alpha_P(0) = 1.08$ (see Donnachie & Landshoff (1992)). Moreover, $\alpha_P(t)$ is not independent of the nature of the scattering particles. This is because, in QCD, the magnitude of $\bar{\alpha}_s$ depends upon the typical size of those particles.

One of the consequences of this is that the unitarity bound of Froissart (1961) and Martin (1963) which tells us that cross-sections cannot grow with s faster than $\ln^2 s$, will be very rapidly violated. We return to the question of the restoration of unitarity in the final chapter.

3. The spectrum of singularities of the Mellin transform is the same for $\mathbf{q}^2 = 0$ as for $\mathbf{q}^2 \neq 0$, i.e. there appears to be no t-dependence of the Pomeron trajectory.

4. Factorization of the amplitude into the product of couplings of the Pomeron to the two incoming hadrons and a Pomeron amplitude only occurs *inside* an integral over transverse momentum, i.e. the integrand of the $\mathbf{k_1}, \mathbf{k_2}$ integrals factorizes into two impact factors and a Pomeron amplitude as shown in Eq.(4.36).

5. The quark-counting rule (Landshoff & Polkinghorne (1971)), which tells us that the coupling of a Pomeron to hadrons is proportional to the number of valence quarks inside the hadron, does not appear to be obeyed. This is because both diagrams of Fig. 4.4 need to be considered in order to have an impact factor which vanishes when $\mathbf{k_1} \to 0$ so that the amplitude is infra-red finite. The graph of Fig. 4.4(b) clearly violates this quark-counting rule since the two sides of the ladder couple to different quarks inside the hadron. However, if Mueller & Tang's prescription is used then it turns out that in certain kinematic regions (e.g. for large t diffractive dissociation processes) the amplitude is dominated by the contribution to the impact factor from Fig. 4.4(a) and is therefore consistent with quark counting.

Analysis of the interface between the soft and hard Pomerons within the context of QCD still presents a challenge. Nevertheless the object that we have been describing so far (the hard Pomeron) should be observable in processes for which the kinematics justifies the use of perturbation theory. We shall turn to a detailed study of the phenomenological implications of this hard Pomeron in Chapters 6 and 7.

4.7 Higher order corrections

So far, all our calculations have been performed in the leading logarithm approximation. In other words we have taken the leading term in an expansion in $1/\ln s$. In particular, we have noted that the leading term in this expansion gives a leading behaviour $s^{\omega_0}/\sqrt{\ln s}$, where ω_0 is the position of the leading singularity in the Mellin transform of the colour singlet exchange amplitude, and is $\mathcal{O}(\alpha_s)$. It is perfectly possible that the sub-leading terms could

sum to give $s^{\omega_1}/(\ln s)^{3/2}$, where ω_1 is also $\mathcal{O}(\alpha_s)$. We see that, for each order in α_s, this expression is suppressed by a power of $\ln s$ relative to the leading logarithm expansion, but if $\omega_1 > \omega_0$ then the summation of the sub-leading logarithms will dominate at sufficiently large s. That this does not happen is an 'act of faith' based on the assumption that $1/\ln s$ is a good expansion parameter and that the leading term should therefore dominate at large s.

Furthermore, the problem of the violation of unitarity mentioned in the preceding section is, as pointed out by Bartels (1980), closely linked with the sub-leading logarithm contributions. The leading $\ln s$ amplitude is obtained by considering cut ladders where the only intermediate states considered are those consisting of gluons radiated off a single reggeized gluon. However, unitarity relates the imaginary part of the amplitude to the sum over *all* possible intermediate states, including those that cannot be produced via colour octet exchange. Thus the leading logarithm approximation does not lead to a unitary amplitude.

It is therefore clear that a full analysis of the sub-leading $\ln s$ contribution is very important for a complete understanding of the perturbative Pomeron.

If we look at all the places where we have made approximations valid *only* for leading logarithms: the multi-Regge kinematic regime which requires $\rho_i \gg \rho_{i+1}$, $|\lambda_{i+1}| \gg |\lambda_i|$ as we go down the ladder; the eikonal approximation for the coupling of soft gluons; the absence of fermion loops; the domination of ladders with reggeized gluons in their vertical lines; etc., we can immediately appreciate that extracting the sub-leading $\ln s$ contribution to the colour singlet exchange amplitude is a formidable task.

Nevertheless, considerable progress has been made both in the systematic calculation of the next-to-leading logarithmic corrections to colour singlet exchange and in the construction of a theory which is unitary. To detail this progress would fill another text book and so we limit ourselves here to a brief chronology of the progress that has been made. Our aim is to provide the reader with a broad overview of the area of sub-leading corrections which will provide a platform for further detailed study.

There are essentially two main lines of research which define the progress that has been made in understanding the corrections

to the BFKL equation. The first line that we shall discuss is motivated by the desire to ensure that the theory be unitary, whilst the second is motivated by the need to compute all the next-to-leading logarithmic corrections to the BFKL equation.

The first attempts to correct the BFKL equation to bring it in line with unitarity date back to Bartels (1980) and Gribov, Levin & Ryskin (1983). Bartels considered the T-matrix for $m \rightarrow n$ scattering. Starting from the lowest order elements (i.e. t-channel exchange of a single reggeized gluon) one is able, using the (s-channel) unitarity relation of Eq.(1.1), to compute the matrix elements at the next order. For example, feeding the lowest order $2 \rightarrow n$ matrix element into the right hand side of Eq.(1.1) leads to the $2 \rightarrow 2$ matrix element also at lowest order (for octet exchange) or the $2 \rightarrow 2$ matrix element at the next order (for singlet exchange). The former is the bootstrap relation we used to prove the reggeization of the gluon in Chapter 3, whilst the latter is none other than the exchange of a BFKL Pomeron.[†] An iterative process can be built up, whereby the higher order corrections are computed from the lower orders in order to fulfil the demands of unitarity. The higher order corrections obtained in this way correspond to a minimal subset of higher order corrections which is determined by the requirements of unitarity. The graphs which constitute this minimal subset are those with the exchange of n reggeized gluons in the t-channel, as in Fig. 4.5, i.e. included are all those graphs which have the Reggeons interacting pairwise via the exchange of gluon rungs (the interaction being described by the BFKL kernel). Clearly, there are many other corrections which are not included in this minimal subset. For example, any graph which does not conserve the number of Reggeons in the t-channel is beyond this approximation. The transition of two Reggeons to four Reggeons has been studied in the papers by Bartels (1993a,b), Bartels & Wüsthoff (1995) and Bartels, Wüsthoff & Lipatov (1995). This work constitutes the development of the original 'fan diagram' calculations (Gribov, Levin & Ryskin (1983) and Mueller & Qiu (1986)) so as to account for

---

[†] Following Bartels, we have referred to this as the next order contribution since the even signature factor associated with the Pomeron exchange is suppressed by one power of α_s relative to the odd signature exchange of the reggeized gluon.
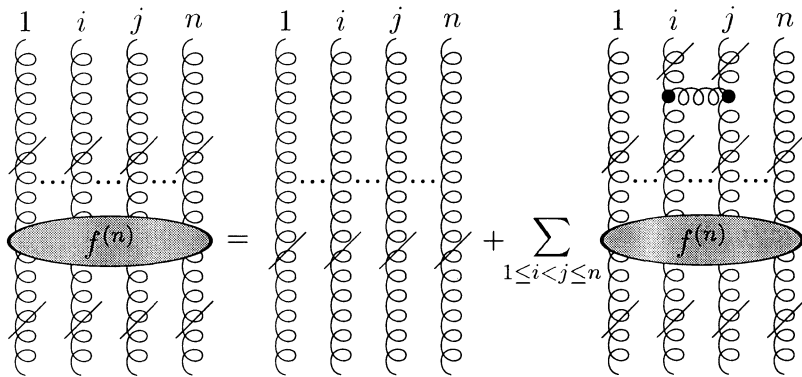
Fig. 4.5. Equation determining the evolution of the n-Reggeon state.

the full Regge kinematics.

Following Bartels (1980), Kwiecinski & Praszalowicz (1980) studied the specific case of the exchange of three reggeized gluons in an overall colour singlet state and with odd charge conjugation, i.e. the odderon. Although the integral equation describing the evolution of the n Reggeon state can easily be written (see Fig. 4.5), its solution is rather more difficult to extract. Significant progress has been made in the papers by Lipatov (1990, 1993, 1994), Kirschner (1994), Korchemsky (1995, 1996) and Faddeev & Korchemsky (1995), where a number of remarkable properties of these colour singlet Reggeon compound states have been established. We shall discuss unitarization corrections further in the final chapter.

The program of computing the next-to-leading logarithmic corrections to the BFKL equation was started in the papers by Lipatov & Fadin (1989a,b), where the leading logarithm tree level amplitudes were corrected to account for the relaxation of the Regge kinematics (i.e. strong ordering of Sudakov components) to the so-called **quasi-multi-Regge kinematics**. The radiative corrections (i.e. quark and gluon loop contributions) to the basic vertices (Reggeon–Reggeon–particle and particle–particle–Reggeon) were computed in the papers by Fadin & Fiore (1992), Fadin & Lipatov (1992, 1993), and Fadin, Fiore & Quartarolo (1994a,b). The

two-loop corrections to the gluon Regge trajectory were computed
by Fadin, Fiore & Quartarolo (1996) and Fadin, Fiore & Kotsky
(1996). The final element which is required to complete this pro-
gramme of work is to compute the amplitudes for the production
of a pair of quarks or gluons in the quasi-multi-Regge kinematics
(i.e. the Reggeon–Reggeon–particle–particle vertices which occur
due to the relaxation of the strong ordering) and this was under-
taken by Fadin & Lipatov (1996). The cancellation of infra-red di-
vergences is expected to occur between the real and virtual graphs
and has been demonstrated explicitly for the fermion contribution
in Fadin & Lipatov (1996). The ultra-violet divergences, which oc-
cur due to the presence of the radiative corrections, do not cancel
and are renormalized into the running of the QCD coupling.

Considerable progress in understanding the 'scale invariant'
part of the sub-leading corrections has been made by White *et al.*
(see e.g. Corianò & White (1995, 1996) and references therein).
Their programme makes use of the simplifications which are af-
forded when one computes amplitudes using the t-channel ana-
logue of Eq.(1.1) (i.e. one considers discontinuities in the t-channel
rather than the s-channel). The 'Reggeon diagrams' which deter-
mine the sub-leading corrections are then straightforward to clas-
sify and, after utilizing gauge invariance (which is implemented
in the form of a Ward identity) and the property that the am-
plitudes be infra-red finite, completely calculable. The property
of infra-red finiteness leads to the fact that only the infra-red or
'scale invariant' parts of the sub-leading corrections are calculated
exactly, e.g. this approach is not able to generate the radiative cor-
rections which lead to the renormalization of the QCD coupling.
However, in the lowest order the method reproduces the complete
BFKL equation.

Before leaving our resumé on the progress made in computing
the sub-leading corrections to the leading logarithm approxima-
tion, let us note that significant progress has been made in the
construction of an effective action which can be derived directly
from the original action of QCD but which is appropriate in the
high energy limit. It is the hope that such an action will be useful
in simplifying the calculation of multi-Reggeon Green functions
due to the fact that unimportant degrees of freedom have been
eliminated (recall that QCD at high energies is concerned essen-

tially with dynamics only in the transverse plane). We refer the interested reader to the papers by Lipatov (1991, 1995), Verlinde & Verlinde (1993) and Kirschner, Lipatov & Szymanowski (1994).

4.8 Summary

• The Pomeron in leading logarithm approximation is obtained by considering colour singlet ladder diagrams whose vertical lines are reggeized gluons with couplings to the gluon rungs given by the effective vertices, Γ.

• The integral equation for the Pomeron (the BFKL equation) is obtained in the same way as the integral equation for the reggeized gluon, but with different colour factors.

• The Pomeron has even signature. In leading logarithm approximation the amplitude is purely imaginary and is suppressed by one power of α_s relative to the reggeized gluon.

• The integral equation is solved for the case of zero momentum transfer by finding the eigenfunctions of the kernel, $\mathcal{K}_0$, given by Eq.(4.18), and their corresponding eigenvalues.

• The eigenvalues are continuous, depending on a discrete variable, n, and a continuous variable, ν. This leads to a cut rather than a pole in the Mellin transform of the Pomeron amplitude, with a branch point at ω_0, given by Eq.(4.31). The leading logarithm behaviour is

$$s^{1+\omega_0}/\sqrt{\ln s}.$$

• The colour singlet exchange amplitude corresponding to the Pomeron (2 gluons → 2 gluons) is free from infra-red divergences.

• The remaining infra-red divergence (which arises from the integration over the transverse momenta of the external gluons) is removed by taking a convolution of the Pomeron with impact factors. The impact factors determine the coupling of the Pomeron to colour singlet hadrons and necessarily vanish when the transverse momentum of any of the gluon legs vanishes.

• The BFKL equation can also be solved for non-zero momentum transfer but it is first necessary to perform a two-dimensional Fourier transform and to work in impact parameter space rather than with the transverse momenta of the external gluons. The

spectrum of eigenvalues is identical to that for zero momentum transfer.

• Some considerable progress has been made in calculating higher order corrections to the perturbative Pomeron, but a complete summation of all sub-leading $\ln s$ contributions has not yet been achieved.

4.9 Appendix

In this appendix we outline the derivation of Eq.(4.47) which gives the BFKL equation in impact parameter space. Firstly let us define

$$\hat{f}(\omega, \mathbf{k_1}, \mathbf{k_2}, \mathbf{q}) = \frac{f(\omega, \mathbf{k_1}, \mathbf{k_2}, \mathbf{q})}{\mathbf{k_2^2}(\mathbf{k_1} - \mathbf{q})^2},$$

so that $\tilde{f}(\omega, \mathbf{b_1}, \mathbf{b_1'}, \mathbf{b_2}, \mathbf{b_2'})$ defined in Eq.(4.46) is actually the two-dimensional Fourier transform of $\hat{f}(\omega, \mathbf{k_1}, \mathbf{k_2}, \mathbf{q})$. The BFKL equation (Eq.(4.16)) then becomes

$$\mathbf{k_1^2}(\mathbf{k_1} - \mathbf{q})^2 \omega \hat{f}(\omega, \mathbf{k_1}, \mathbf{k_2}, \mathbf{q}) = \delta^2(\mathbf{k_1} - \mathbf{k_2}) + \frac{\bar{\alpha}_s}{2\pi} \int d^2\mathbf{k'}$$

$$\left\{ -\mathbf{q}^2 \hat{f}(\omega, \mathbf{k'}, \mathbf{k_2}, \mathbf{q}) + \frac{\mathbf{k_1^2}}{(\mathbf{k_1} - \mathbf{k'})^2} \left[(\mathbf{k'} - \mathbf{q})^2 \hat{f}(\omega, \mathbf{k'}, \mathbf{k_2}, \mathbf{q}) \right. \right.$$

$$\left. - \frac{\mathbf{k_1^2}(\mathbf{k_1} - \mathbf{q})^2}{[\mathbf{k'}^2 + (\mathbf{k'} - \mathbf{k_1})^2]} \hat{f}(\omega, \mathbf{k_1}, \mathbf{k_2}, \mathbf{q}) \right]$$

$$+ \frac{(\mathbf{k_1} - \mathbf{q})^2}{(\mathbf{k_1} - \mathbf{k'})^2} \left[\mathbf{k'}^2 \hat{f}(\omega, \mathbf{k'}, \mathbf{k_2}, \mathbf{q}) \right.$$

$$\left. \left. - \frac{\mathbf{k_1^2}(\mathbf{k_1} - \mathbf{q})^2}{[(\mathbf{k'} - \mathbf{q})^2 + (\mathbf{k'} - \mathbf{k_1})^2]} \hat{f}(\omega, \mathbf{k_1}, \mathbf{k_2}, \mathbf{q}) \right] \right\} . \quad (A.4.1)$$

Now we note the following Fourier transforms (F.T.):

$$-\partial_{\mathbf{b_1}}^2 \, \tilde{f}(\omega, \mathbf{b_1}, \mathbf{b_1'}, \mathbf{b_2}, \mathbf{b_2'}) = \text{F.T.} \left\{ \mathbf{k'}^2 \hat{f}(\omega, \mathbf{k'}, \mathbf{k_2}, \mathbf{q}) \right\}$$

$$-\partial_{\mathbf{b_1'}}^2 \, \tilde{f}(\omega, \mathbf{b_1}, \mathbf{b_1'}, \mathbf{b_2}, \mathbf{b_2'}) = \text{F.T.} \left\{ (\mathbf{k'} - \mathbf{q})^2 \hat{f}(\omega, \mathbf{k'}, \mathbf{k_2}, \mathbf{q}) \right\}$$

(and identical expressions with $\mathbf{k'}$ replaced by $\mathbf{k_1}$), and

$$-(\partial_{\mathbf{b_1}} + \partial_{\mathbf{b_1'}})^2 \, \tilde{f}(\omega, \mathbf{b_1}, \mathbf{b_1'}, \mathbf{b_2}, \mathbf{b_2'}) = \text{F.T.} \left\{ \mathbf{q}^2 \hat{f}(\omega, \mathbf{k'}, \mathbf{k_2}, \mathbf{q}) \right\},$$

so that

$$-\int d^2\mathbf{k}'\mathbf{q}^2\hat{f}(\omega,\mathbf{k}',\mathbf{k_2},\mathbf{q})$$

is the (inverse) Fourier transform of

$$(2\pi)^2\delta^2(\mathbf{b_1}-\mathbf{b_1'})(\partial_{\mathbf{b_1}}+\partial_{\mathbf{b_1'}})^2\tilde{f}(\omega,\mathbf{b_1},\mathbf{b_1'},\mathbf{b_2},\mathbf{b_2'})$$

$((\mathbf{b_1}-\mathbf{b_1'})$ is the impact parameter conjugate to $\mathbf{k_1})$.

We have shown in Section 4.3 that the integral

$$\int \frac{\mathbf{k_1^2}\,d^2\mathbf{k}'}{(\mathbf{k}'-\mathbf{k_1})^2[\mathbf{k'^2}+(\mathbf{k}'-\mathbf{k_1})^2]}=\int_0^{\mathbf{k_1^2}}\frac{d^2\mathbf{k}'}{\mathbf{k'^2}}$$

(plus integrals which cancel). This is infra-red divergent and so we regularize it by writing it as

$$\lim_{\lambda\to0}\int_0^{\mathbf{k_1^2}}\frac{d^2\mathbf{k}'}{(\mathbf{k'^2}+\lambda^2)}=\pi\ln\left(\frac{\mathbf{k_1^2}+\lambda^2}{\lambda^2}\right);$$

this is the (inverse) Fourier transform of

$$\lim_{\lambda\to0}\frac{1}{(\mathbf{b^2}+\lambda^2)}.$$

The Fourier transform of the product of two functions $g(\mathbf{k}),h(\mathbf{k})$ is given by the convolution

$$\int d^2\mathbf{k}'g(\mathbf{k}')h(\mathbf{k}')e^{i\mathbf{b}\cdot\mathbf{k}'}=\frac{1}{(2\pi)^2}\int d^2\mathbf{c}\tilde{g}(\mathbf{c})\tilde{h}(\mathbf{b}-\mathbf{c}).$$

For example,

$$\int\frac{d^2\mathbf{c}}{(\mathbf{b}-\mathbf{c})^2}\tilde{g}(\mathbf{c})$$

$$=\text{ F.T.}\left\{\int d^2\mathbf{k}'\frac{\mathbf{k_1^2}}{(\mathbf{k_1}-\mathbf{k}')^2[\mathbf{k'^2}+((\mathbf{k}'-\mathbf{k_1})^2]}g(\mathbf{k_1})\right\}\quad(\text{A}.4.2)$$

and, conversely,

$$\int d^2\mathbf{c}\frac{(\mathbf{b_1}-\mathbf{b_1'})^2}{(\mathbf{b_1}-\mathbf{c})^2\left[(\mathbf{b_1}-\mathbf{c})^2+(\mathbf{b_1'}-\mathbf{c})^2\right]}\tilde{g}(\mathbf{b_1},\mathbf{b_1'})$$

$$=\text{ F.T.}\left\{\int\frac{d^2\mathbf{k}'}{(\mathbf{k}'-\mathbf{k_1})^2}g(\mathbf{k}')\right\}.\quad(\text{A}.4.3)$$

(In Eq.(A.4.3) we shift the integration variable on the left hand side to $(\mathbf{c}-\mathbf{b_1})$ and again use the fact that $\mathbf{b_1}-\mathbf{b_1'}$ is the variable conjugate to $\mathbf{k_1}$.

Inserting $\mathbf{k}_1^2 f(\omega, \mathbf{k}_1, \mathbf{k}_2, \mathbf{q})$ or $(\mathbf{k}_1 - \mathbf{q})^2 f(\omega, \mathbf{k}_1, \mathbf{k}_2, \mathbf{q})$ for $g(\mathbf{k}_1)$ in Eq.(A.4.2) where necessary, and likewise $\mathbf{k}'^2 f(\omega, \mathbf{k}', \mathbf{k}_2, \mathbf{q})$ or $(\mathbf{k}' - \mathbf{q})^2 f(\omega, \mathbf{k}', \mathbf{k}_2, \mathbf{q})$ for $g(\mathbf{k}')$ in Eq.(A.4.3) and recalling that an extra power of $\mathbf{k}_1^2$ or $(\mathbf{k}_1 - \mathbf{q})^2$ can be obtained by acting on the left with $-\partial_{\mathbf{b}_1}^2$ or $-\partial_{\mathbf{b}_1'}^2$, respectively, the result, Eq.(4.47), follows.

Note that the product terms in Eq.(A.4.1) become convolution terms under the Fourier transform and *vice versa*.